Formation and properties of multivariant assemblies of surface-tethered diblock and triblock copolymers

Michael R. Tomlinson, Jan Genzer*

Department of Chemical and Biomolecular Engineering, North Carolina State University, 911 Partners Way, Raleigh, NC 27695-7905, USA

A B S T R A C T

We present methodologies for fabricating block copolymer assemblies grafted onto flat solid substrates, where each block of the copolymer possesses a systematic and gradual variation of molecular weight as a function of the position on the substrate. We demonstrate the utility of this technique on two case studies. In the first project, we generate surface-tethered poly[(2-hydroxyethyl methacrylate)-*b*-(methyl methacrylate)] (PHEMA-*b*-PMMA) diblock copolymer brushes and study systematically morphological transitions associated with collapsing either the top PMMA or the bottom PHEMA block while keeping the other block solvated. Scanning force microscopy studies of systems having the top block collapsed reveal the presence of either flat (F), or micellar (M) or bicontinuous (BC) morphologies, whose locus in the phase diagram agrees with theoretical predictions and results of computer simulations. The second case study demonstrates the extension of the deposition method to the case of surface-anchored triblock copolymer brushes. Specifically, we present results pertaining to the formation of poly[(2-hydroxyethyl methacrylate)-*b*-(methyl methacrylate)-*b*-(dimethylaminoethyl methacrylate)] brushes with independent variation of all three block lengths.

© 2008 Elsevier Ltd. All rights reserved.

1. Introduction

Modification of surfaces with chemically anchored polymers has been the topic of numerous studies over the past few years. Ingenious chemical and assembly routes have been conceived and developed that are based on creating surface-grafted polymer assemblies by either deposition of polymer chains onto the surface from solution or melt (so-called "grafting onto" methodologies) or by polymerizing macromolecules directly from the substrate (so-called "grafting from" methodologies) [1–4]. Substrate-anchored polymer assemblies, henceforth referred to as "polymer brushes",[1] offer unprecedented means of controlling the physico-chemical characteristics of substrates via adjusting their length (or equivalently molecular weight), density on the substrate (so-called grafting density), and chemical composition. As demonstrated by many research groups, controlling these material attributes

endows polymer brushes with unique means of adjusting the spatio-temporal character of the substrates [5].

To this end, one of the rapidly growing areas, in which polymer brushes have played a pivotal role, involves generating "smart"/responsive surfaces [6]. In a broad sense, responsive materials involve surfaces, which can adapt their physico-chemical characteristics in response to an external stimulus, *i.e.*, chemical, electrical, or mechanical [7]. Applying these external forces results typically in a dramatic rearrangement of surface-anchored macromolecules resulting in variations of wettability, topography, and morphology [8–10]. During the past few years several researchers have reported on tailoring the topology of soft material surfaces by utilizing surface-confined copolymers in conjunction with selectively swelling one of the blocks, while collapsing the other block. For instance, in their pioneering work, Zhao and coworkers demonstrated conclusively that selective swelling and collapse of poly(styrene-*b*-methyl methacrylate) brush blocks produced variable and switchable surface topologies [11,12]. This simple and yet very powerful method of tailoring substrate topologies has led to exciting developments in utilizing surface-grafted polymers as potential "soft vehicles" capable of moving nano-sized objects [13–15]. Application of selectively swollen/collapsed copolymer brushes in such applications requires knowledge of how the development of the topographical features depends on the lengths of the individual blocks and the degree of collapse. Because of the large number of independent variables involved in such studies it is not

---

* Corresponding author. Tel.: +1 919 515 2069; fax: +1 919 515 3465.
   E-mail addresses: m.tomlinson@alumni.ncsu.edu (M.R. Tomlinson), jan_genzer@ncsu.edu (J. Genzer).

   [1] We note that this nomenclature may be somewhat confusing. Strictly speaking, "polymer brushes" denote substrate-anchored assemblies of macromolecules, whose conformation is greatly stretched away from the Gaussian coil. In this paper, we use the term "polymer brush" to represent the more general case of a macromolecule chemically attached to a substrate without implying any particular conformational arrangement.

feasible to probe these effects using individual samples, which all possess a fixed length of the two copolymer blocks. Instead, a more efficient and systematic method is required that would allow one to explore and map out the entire parameter space using tailored brush systems [16]. This task can be accomplished by fabricating brush assemblies with a continuous variation of the physico-chemical characteristics of the substrates anchored polymers. During the past few years, methods have been developed that enable the fabrication of polymer arrays with spatial variation of properties, including grafting density [17–23], length [21,24], and composition [25–27]. Some of those techniques have been reviewed recently [28–31].

In this paper we expand on our previous report [32] and present a method for generating A-*b*-B diblock copolymer assemblies with orthogonal variation of the lengths of both blocks on a single substrate and study systematically the dependence of surface topology of the two blocks after selectively collapsing either the top or the bottom block. We demonstrate that our findings are in very good qualitative agreement with theoretical predictions of Zhulina et al. [33,34] and Balazs et al. [35] and simulated annealing study of Yin and coworkers [36]. In addition, we demonstrate the extension of the methodology leading to the production of diblock copolymer brush assemblies as well as A-*b*-B-*b*-C triblock copolymer assemblies with independent length variation of each of the three blocks. Additionally we outline applications of such structures.

2. Experimental details

2.1. Deposition of the polymerization initiator

After chilling 20 ml of anhydrous toluene (dried over MgSO$_4$) to approximately −10 °C, 2.5 μl of (11-(2-bromo-2-methyl)propionyloxy)undecyl-trichlorosilane (BMPUS) was added, which was synthesized by following previous reports [37]. Silicon wafers (Silicon Valley Microelectronics), cut into 5 cm × 5 cm squares (wafer orientation [100]) or equilateral triangles having an edge length of 5 cm (wafer orientation [111]), were exposed for 30 min to UV/ozone treatment in order to generate a large number of surface-bound hydroxyl groups. The wafers were then added to the toluene-solution of BMPUS and allowed to sit at −10 °C for 6 h, after which time they were removed, rinsed copiously with toluene, and sonicated in pure toluene for 1–30 min (depending on the strength of the sonicator). The substrates, covered with monolayers of BMPUS were stored in a dry box for use within a two-week period.

2.2. Surface-initiated polymerization

The polymerization was carried out at 25 °C for all monomer systems, including methyl methacrylate (MMA) (99%, ACROS), 2-hydroxyethyl methacrylate (HEMA) (98%, ACROS), and dimethylaminoethyl methacrylate (DMAEMA) (98%, Aldrich). Acetone (HPLC grade, Fisher Scientific), methanol (HPLC grade, Fisher Scientific), and DI water were used as co-solvents for each monomer. Solvents and monomers were sparged with nitrogen prior to polymerizations in order to remove any oxygen. Polymerizations of MMA and DMAEMA were carried out using 50 ml of monomer, 46 ml (= 1.136 mol) of methanol, 10.0 ml of deionized water, 3.0 g bipyridine (= 1.9 × 10^{-2} mol), and 9.6 × 10^{-3} mol of CuCl + CuCl$_2$ (usually in the molar ratio of 20:1) [38,39]. In order to generate linear (uncross-linked) PHEMA brushes, we follow the procedure suggested in [40]. The polymer brush gradient-based substrates were prepared in a custom-made polymerization chamber (*cf.* Fig. 1). The chamber was continuously purged with nitrogen in order to avoid oxygenation of the macroinitiator or monomer/catalyst solutions. BMPUS-treated wafers were fixed onto a "dipping" sample holder able to control the longitudinal position of the wafer in a discrete or semi-continuous manner to less than 0.1 mm. Monomer/catalyst solutions were loaded into beakers within the chamber on a moving carousel that could be positioned
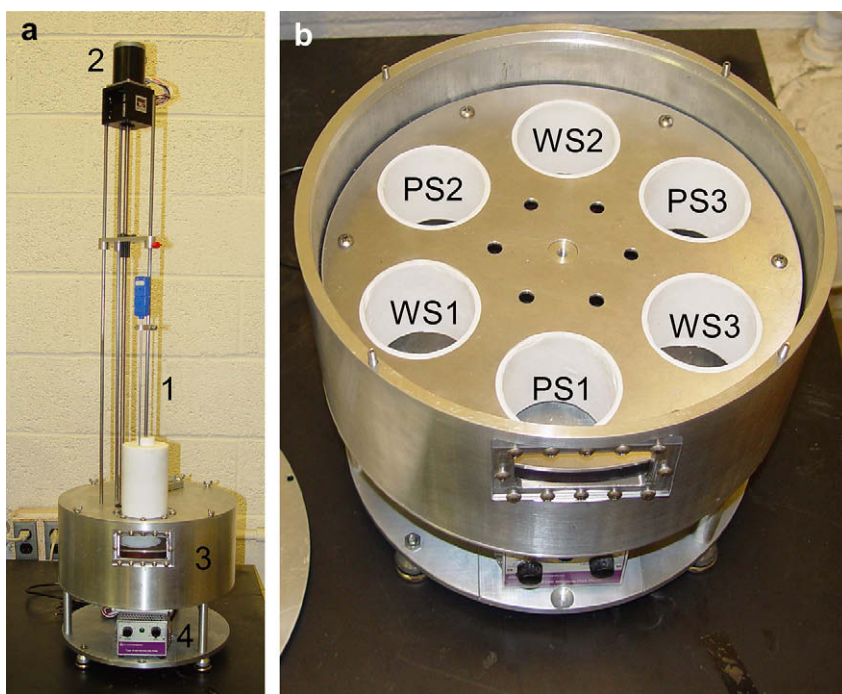

Fig. 1. (a) Picture of a dipping apparatus for preparing polymer gradient assemblies described in this paper. The sample is placed into a holder whose vertical motion is adjusted by a rod (1) attached to a stepper motor (2), which enables sample insertion to and from a reaction chamber (3) containing a carousel with various polymerization solutions and washing stations (*cf.* Fig. 1b). The solution underneath the dipping arm can be heated and stirred (4) (b) Details of the carousel holding up to 3 polymerization solutions (PS1–PS3), containing a mixture of a monomer, solvent, ligand, Cu$^{(I)}$X and Cu$^{(II)}$X salts, and 3 washing stations (WS1–WS3).

below the sample. In this manner, multiple monomers could be used for a single sample run without exposing the sample or solutions to external oxygen. After each polymerization step, the wafer was immersed multiple times into a methanol solution containing dissolved bipyridine/CuCl$_2$ complex. This step was necessary in order to remove any adsorbed (but unreacted) monomer and to bring any active chains into their dormant state. Both the carousel and dipping mechanism were controlled via a computer program and a stepper motor/controller (Applied Motion Products).

2.3. Analysis of polymer properties

Position-dependent thickness measurements were performed with a variable-angle spectroscopic ellipsometer (VASE, J.A. Woollam). The spot size was 0.5 mm and a constant refractive index of 1.50 was used for all polymer layers, introducing an error <3% of dry layer thickness. The thickness was measured after synthesizing each individual block. In our previous publication we have established that removing the sample from polymerization solution and keeping it in air for a few hours did not adversely affect the ability of the block to act as a macroinitiator, *i.e.*, polymerization of another block on top of the macroinitiator could be carried out [41]. The topography of surface-tethered diblock copolymer brushes after collapsing either the top or the bottom block and after vitrification was determined from tapping mode scanning force microscopy (SFM) using Nanoscope III (Digital Instruments) at various positions along the substrate.

3. Results and discussion

3.1. Diblock copolymer brushes with variable block lengths

We prepared a surface-tethered block copolymer of poly[(2-hydroxyethyl methacrylate)-*b*-poly(methyl methacrylate)] (PHEMA-

b-PMMA) with gradually varying lengths of both blocks on a single substrate using the method described in Section 2. Specifically, silicon wafers (5 × 5 cm^2) decorated with a BMPUS monolayer were first covered with a gradient in molecular weight of PHEMA by "grafting from" polymerizing 2-hydroxyethyl methacrylate using the dipping method described in Section 2. The orthogonal diblock gradient was formed using the PHEMA-brush covered samples, orienting it such that the PHEMA molecular weight gradient was positioned horizontally and polymerizing methyl methacrylate (MMA) from the PHEMA macroinitiator centers on the substrate. This procedure resulted in a PHEMA-*b*-PMMA diblock copolymer brush with position-dependent lengths of the two blocks on the substrate. Fig. 2 depicts pictorially the technological steps leading to the formation of PHEMA-*b*-PMMA brushes. Also shown is a photograph of the actual specimen (*cf.* Fig. 2d). The data analysis and discussion that follow are based on measurements carried out on two separate specimens.

We used ellipsometry in order to gain detailed information about the molecular properties of the PHEMA and PMMA blocks in the PHEMA-*b*-PMMA brush as a function of the position on the sample. In Fig. 3 we plot the dry thickness maps along the PHEMA-*b*-PMMA specimen. The thickness of each block was determined using ellipsometry after each synthesis step. PHEMA dry thickness increases linearly along the *Y* direction (Fig. 3a) and the PMMA thickness increases linearly in the *X* direction (Fig. 3b). Because the grafting density, σ, of all polymers is approximately equal on the entire specimen, the dry thickness of each block, *h* is directly proportional to its molecular weight, *M*:

$$h = \frac{\sigma M}{\rho N_A}, \tag{1}$$

where ρ and N_A are polymer density and Avogadro's number, respectively [42]. More information about the various copolymer

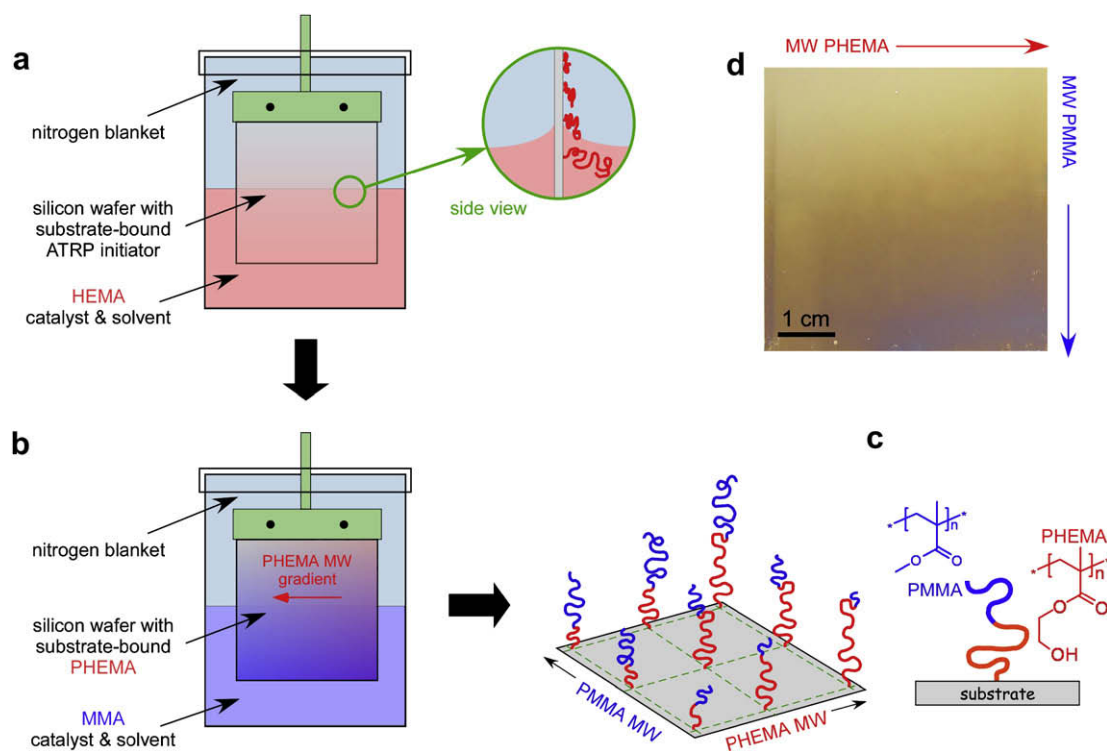**Fig. 2.** (**left**) Method of preparing surface-tethered block copolymer poly[(2-hydroxyethyl methacrylate)-*b*-poly(methyl methacrylate)] (PHEMA-*b*-PMMA) with smoothly varying lengths of both blocks on a single substrate. The procedure consists of first decorating the silicon wafer with a PHEMA brush (a) with a varying length of the polymer using the dipping method. After rotating the sample orthogonally, the PHEMA brush is used as a macroinitiator enabling the polymerization of MMA with a gradual variation of PMMA length (b). The resultant sample (c) comprises poly[(2-hydroxyethyl methacrylate)-*b*-poly(methyl methacrylate)] copolymers with systematic variation of the lengths of both blocks. Part (d) depicts a photograph of the actual sample. The darker colour corresponds to thicker PHEMA-*b*-PMMA layer.
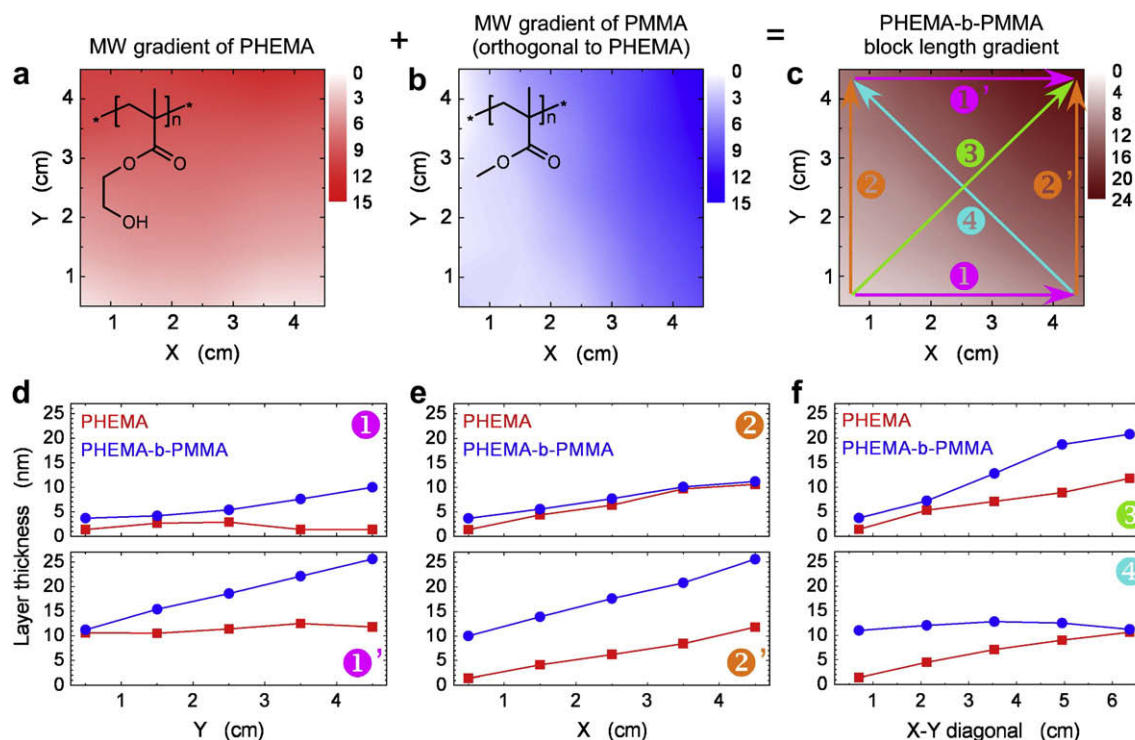
Fig. 3. Dry thickness profiles of PHEMA (a), PMMA (b) and PHEMA-*b*-PMMA (c) MW1/MW2 orthogonal brush (in nm) as a function of the position on the substrate. (d–f) PHEMA (red squares) and total copolymer (blue circles) thicknesses along the directions depicted in the total thickness profile shown in the upper right corner. The lines in parts (d–f) are meant to guide the eye. The thickness error bars are smaller than the size of the symbols. (For interpretation of the references to colour in this figure legend, the reader is referred to the web version of this article.).

compositions can be obtained by plotting the dry thicknesses of the PHEMA and PMMA blocks along the various directions indicated by arrows in Fig. 3c. The horizontally pointing arrows denote copolymers having a constant PMMA length and a linearly increasing PHEMA length. Two cases are highlighted here, copolymers with a short (❶) and long (❶′) PMMA block (Fig. 3d). The vertical arrows depict block copolymers with a linearly varying length of the PMMA block and a constant length of the bottom PHEMA block. As before, we mark the boundary cases involving a short (❷) and long (❷′) PHEMA block (Fig. 3e). The diagonals in Fig. 3c denote copolymers that have: (❸) approximately constant fraction of both blocks but an increased total length, and (❹) those with a constant length but a linearly varying composition (Fig. 3f). Overall, the ellipsometric data confirm that the specimen contains all possible combinations of the lengths of PHEMA and PMMA blocks (up to the upper boundary length of each block).

In order to utilize PHEMA-*b*-PMMA surface-anchored copolymers to systematically map out the influence of the block length on surface morphologies of PHEMA-*b*-PMMA in response to selectively collapsing either the top (PMMA) block or the lower (PHEMA) block of the copolymer the orthogonal gradient specimen was immersed in 40% ethanol/acetone (v/v) solution, a good solvent mixture for both blocks, followed by gradual variation of the solvent quality. In order to collapse the top PMMA block while keeping the bottom PHEMA block solvated, we gradually changed the composition of the solution by adding ethanol, a poor solvent for PMMA (*cf.* Fig. 4). When the content of ethanol in the solution reached ≈90%, the sample was immediately transferred to 100% anhydrous ethanol. In order to vitrify the surface morphology of the PHEMA-*b*-PMMA copolymers and minimize the reordering of the copolymer structures upon drying, the sample was immersed into liquid ethane (freezing point −211 °C, boiling point −88 °C). The cold nonpolar ethane causes the polar PHEMA and PMMA to

collapse and withdraws any solvent left behind. The ethane and the sample were allowed to increase in temperature until the ethanol was absorbed completely by the ethane phase. The sample was then immersed in liquid nitrogen and transferred to a vacuum oven at room temperature. The following "reverse" solvent treatment was designed to swell the entire copolymer chain then selectively collapse the bottom PHEMA block. After immersing the orthogonal gradient specimen in 40% acetone/ethanol (v/v) solution, the solution composition was subsequently gradually changed by adding acetone, a poor solvent for PHEMA (*cf.* Fig. 4). When the
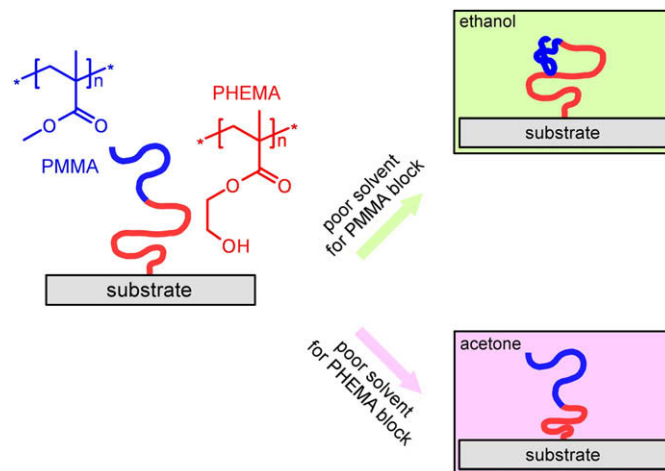

Fig. 4. Schematic of the conformation of poly[(2-hydroxyethyl methacrylate)-*b*-(methyl methacrylate)] (PHEMA-*b*-PMMA) diblock copolymer brush before (**left**) and after exposing to a selective solvent that collapses the top PMMA (**top right**) and bottom PHEMA (**bottom right**) block.

content of acetone in the solution reached $\approx 90\%$, the sample was immediately transferred to 100% anhydrous acetone. In order to vitrify the surface morphology of the PHEMA-*b*-PMMA copolymers and minimize the reordering of the copolymer structures upon drying, the sample was immersed into liquid butane (freezing point $-138\,^{\circ}\text{C}$, boiling point $-0.5\,^{\circ}\text{C}$). Butane was used in place of ethane due to the freezing point of acetone being too high to use ethane. The butane and the sample were allowed to increase in temperature until the acetone was liquid and miscible with the butane phase. The sample was then immersed in liquid nitrogen and transferred to a vacuum oven at room temperature.

More than a decade ago, Zhulina and coworkers studied the swelling of surface-tethered copolymers using selective solvents using self-consistent field (SCF) theory and scaling arguments [33–35]. Their work revealed that grafted copolymers exposed to a solvent that is a theta solvent for the bottom block and a poor solvent for the top block exhibit several distinct morphologies, including, flat (I), pure B pinned micelles (PM-B), A-legged micelles (M-AB), star-like micelles (M-A), and a bicontinuous phase (BAB) (*cf.* Fig. 5). The type of morphology the copolymer adopted depended on the lengths of the individual blocks. Recently, Yin and coworkers [36] extended the work of Zhulina et al. by utilizing a simulated annealing method. Yin et al. explored systematically the effect of solvent quality on either the top or the bottom block of the copolymer, copolymer overall length, and copolymer grafting density. Their results were found to be in accord with the predictions of Zhulina et al. Our sample design is ideally suited for testing the predictions of Zhulina and coworkers and Yin and coworkers. Having copolymers with independent and smoothly varying lengths of each block on a single sample, we can systematically screen the entire parameter space in a reproducible and fast manner without using internal standards. Moreover, we can make a direct comparison to the diagram presented by Zhulina et al. by recognizing that σN, the coordinate system employed in the simulation work translates directly to the coordinate adopted in our system (*i.e.*, $\sigma N \approx h$, *cf.* Eq. (1)). In order to explore the effect of solvent quality on the composition of the PHEMA-*b*-PMMA

copolymer, the samples were exposed to the various selective solvents described earlier. The sample surface morphology was then probed with tapping mode scanning force microscopy (SFM). SFM images were taken from 25 equally spaced locations on the sample.

We commence with describing results obtained after selective solvent treatment designed to collapse the top PMMA block. In Fig. 6 we plot the morphology diagram based on multiple SFM scans collected from several areas on two different PHEMA-*b*-PMMA orthogonal samples. Fig. 7 depicts selected SFM scans taken along directions indicated by the dashed regions in Fig. 6. Specifically, in Fig. 6 we plot morphology development for samples having approximately constant PHEMA block length and increasing PMMA block length for three different PHEMA lengths (❶ through ❸; increasing from ❶ to ❸) as well as those from specimens with nearly constant PMMA block length and increasing PHEMA block length (❹). Our results, which are in excellent qualitative agreement with the predictions of Zhulina and coworkers (*cf.* Fig. 5), show a definite trend in the morphologies of the PHEMA-*b*-PMMA copolymer that range from flat (F) to "floating micelles" to "aggregating micelles" (M) and finally to a bicontinuous phase (BC), which we have detected to be "honeycomb"-like shaped. From the work of Zhulina et al. it is not apparent whether the transitions from micellar to bicontinuous occur rapidly or gradually [34]. While separate categories of the individual phases (F, M, BC) appear in the SFM images quite clearly, the transitions were found to occur, however, very gradually as molecular weight was increased. To that end, in the phase diagram (*cf.* Fig. 6), we have also included an M/BC (micellar/bicontinuous transitional) phase to demark a region in which micelles were partially aggregating as well as transition between the micelles and the bicontinuous phase (M/BC).

The SFM results can be broken down into two basic effects: (i) the increase in size of the micelles (dependent primarily on the PHEMA block length) and (ii) the ability of chains to aggregate (dependent primarily on the PMMA block length). The transition labeled ❶ in Fig. 6 represents the region of relatively short PHEMA and increasing PMMA blocks. Upon viewing the images sequentially from top left to bottom right we see a flat (F) morphology, two micellar images (M), two images in the aggregating micellar region (M/BC), and finally one that appears to be fully bicontinuous (BC). The PHEMA block is small and so we believe that the confinement causes the transitions to occur sooner and have smaller features. Transitions ❷ and ❸ in Fig. 6 exhibit similar patterns. Two main
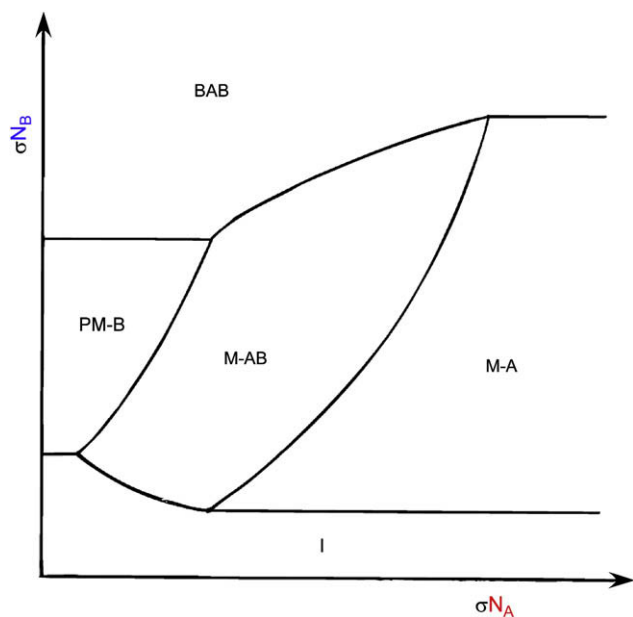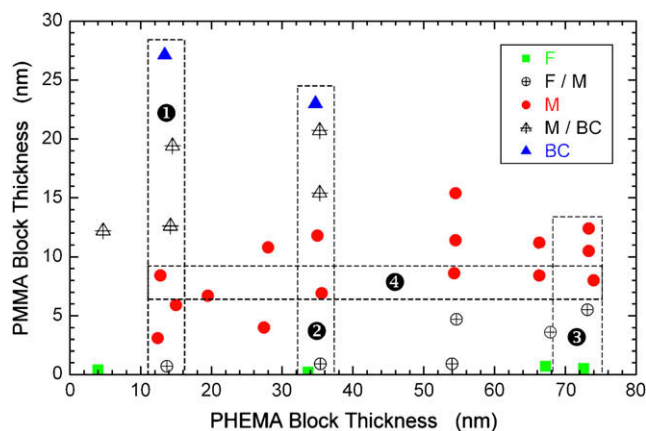

Fig. 5. Morphology diagram of an A–B diblock copolymer brush anchored to a substrate with the top block (B) collapsed. The morphology diagram, generated using numerical self-consistent field theory, reveals the existence of 5 distinct morphologies: flat (I), pure B pinned micelles (PM-B), A-legged micelles (M-AB), star-like micelles (M-A), and a bicontinuous phase (BAB). Redrawn from Ref. [34].

Fig. 6. Phase diagram for ethanol-quenched PHEMA-*b*-PMMA brushes plotted as a function of the PHEMA and PMMA block lengths expressed in terms of dry PHEMA (h_{PHEMA}) and PMMA (h_{PMMA}) thickness. The phase diagram reveals the existence of flat (F, filled squares), micellar (M, filled circles), and bicontinuous (BC, filled triangles) morphologies. The F/M (crossed circles) and M/BC (crossed triangles) regions denote samples, whose morphology could not be identified unambiguously.
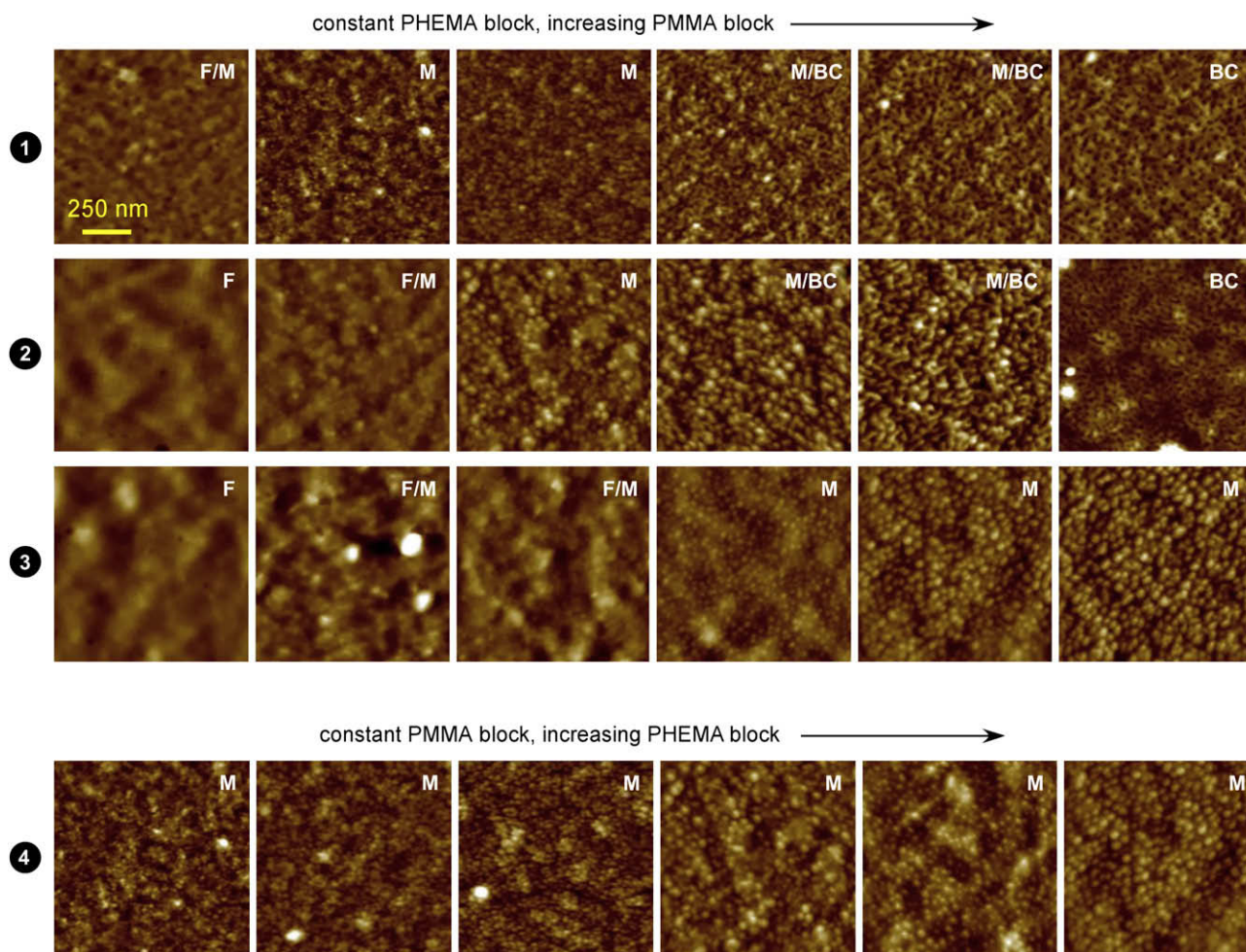
constant PHEMA block, increasing PMMA block ⟶

constant PMMA block, increasing PHEMA block ⟶

Fig. 7. Representative topographies of ethanol-quenched PHEMA-*b*-PMMA brushes collected by scanning force microscopy on various positions on the sample corresponding to different combinations of the PHEMA and PMMA block the substrate as denoted by the dashed regions ❶, ❷, ❸, and ❹, in Fig. 6. Specifically, the top panels show specimens with approximately constant PHEMA block length and increasing PMMA block length for three different PHEMA lengths (increasing from ❶ to ❸, *cf.* Fig. 6). The bottom panel presents images collected from samples with nearly constant PMMA block length and increasing PHEMA block length. The size of each image is $1 \times 1 \ \mu m^2$. The height scale of the SFM images ranges from 0 (dark brown) to 30 nm (white). (For interpretation of the references to colour in this figure legend, the reader is referred to the web version of this article.).

differences emerge. First there is an appearance of floating micelles (most clearly seen in the path ❸), or micelles that are isolated and are located just beneath the surface of the PHEMA layer. Second, the structural features seen are enlarged. Due to the increased freedom, each PMMA chain is being tethered by a longer PHEMA bottom block. In other words, chains are allowed to aggregate to form micelles with larger micellar cores producing larger features. Also, due to increased chain freedom, micellar aggregation to produce a bicontinuous phase occurs more gradually over a longer range of block length. The last transitional line ❹ depicts micelles formed from a relatively constant PMMA block length with increasing PHEMA block length. Presumably, the increase in chain freedom causes these micelles to aggregate over a larger area thereby increasing micellar size. These results may be somewhat counter-intuitive as one might expect the micelle size to be more dependent on the PMMA block length since the PMMA composes the core of the micelle. However, when chain mobility, primarily dependent on the PHEMA chain length, is taken into account this finding is understandable. In the region of short PHEMA, the PMMA micellar core is pinned close to the surface.

Upon solvent treatment designed to collapse the bottom PHEMA block a very different morphology was observed. Zhulina and coworkers predicted that upon collapsing the bottom block, the bottom block would form micellar cores while the top block would

exhibit "flower-like" fingers protruding out from the micellar cores [34]. Zhulina's "flower-like" arrangement is seen as a spongy morphology (*cf.* Fig. 8); it is only visible in intermediate regions of the sample. In regions with a short PHEMA block, the morphology appears fairly flat for all PMMA block lengths. Upon increasing the PHEMA block length, the spongy morphology becomes less visible giving away to larger order surface oscillations from the collapsed PHEMA chain. The transition from nearly flat to spongy morphologies is seen as we move along the wafer in the intermediate PMMA block length (dry thickness ≈ 12 nm) region from short to long PHEMA block. The second image from the left in Fig. 8 exhibits the most clear spongy morphology and occurs at block thicknesses of 7–12 nm for PMMA and 40–50 nm for PHEMA. Continued increase in the PHEMA block length brings about a mixed spongy/micellar structure seen in the last image in Fig. 8. We note that the morphologies presented here are also in a very good qualitative agreement with the predictions of Yin and coworkers [36]. We stress, however, that the discussion of morphological transitions based solely on SFM images may not provide the most complete picture of the behavior. To this end, techniques capable of determining the definite structure of the morphological state, such as grazing incidence small X-ray scattering (GSAXS) may be required. We plan to revisit the discussion of the features described thus far in the future with GSAXS. In the meantime, we provide additional
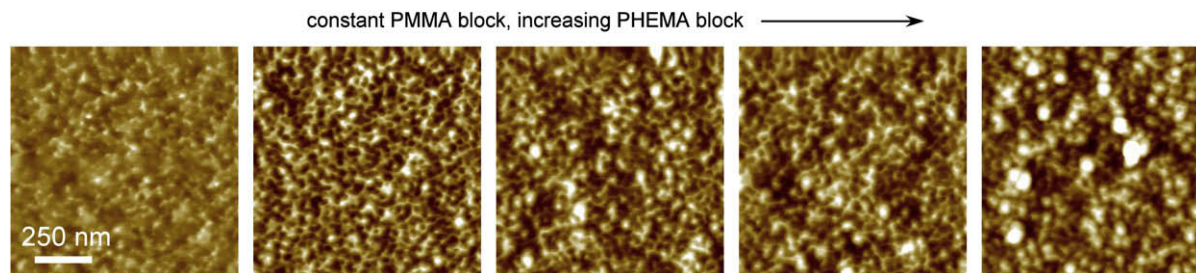
constant PMMA block, increasing PHEMA block ⟶

Fig. 8. Representative scanning force microscopy images on various positions along the substrate on various positions on the acetone-quenched sample having the same length of the PMMA block and increasing length of the PHEMA block (*cf.* direction ❹ in Fig. 6). The size of each image is $1 \times 1 \ \mu m^2$. The height scale of the SFM images ranges from 0 (dark brown) to 30 nm (white). (For interpretation of the references to colour in this figure legend, the reader is referred to the web version of this article.).

characterization of the morphological structures observed on the PHEMA-*b*-PMMA brushes with either the top or the bottom block collapsed using rudimentary wettability tests; those are described next.

Contact angle data can provide complementary information about the chemical nature of the topmost layer of polymer (<1 nm). Though certain error is associated with individual contact angle measurements, our experiments, which involve the acquisition of over 25 measurements per solvent exposure, reveal certain definite trends. It has to be stressed that high surface roughness can, at times, give artificially high or low readings based on the chemical nature of the surface. Specifically, a rough hydrophilic polymer surface (contact angle $< 90°$) may give artificially low readings whereas a more hydrophobic polymer surface (contact angle $> 90°$) may provide a high reading. To ensure this was not the case here, we measured surface roughness at each region on the sample. No significant increase in the surface roughness was detected on the areas of the samples corresponding to the transitional regions between micellar and bicontinuous morphologies. Hence, surface roughness is not expected to greatly affect the differences in the contact angle data.

Clear differences in wettabilities were detected when comparing the surfaces exposed to different solvents (*cf.* Fig. 9).

Fig. 9. Static contact angles of deionized water (DIW) (in deg) measured on various positions along the specimen containing the poly[(2-hydroxyethyl methacrylate)-*b*-(methyl methacrylate)] (PHEMA-*b*-PMMA) diblock copolymer brush after exposing to a selective solvent that collapses the top PMMA (a) and bottom PHEMA (b) block (*cf.* Fig. 4). The static DIW contact angles of PMMA and PHEMA are 75° and 48°, respectively.

Whereas samples having the top PMMA block collapsed produced contact angles of deionized water (DIW) varying from 50° to over 75°, collapsing the bottom PHEMA block yielded a fairly homogeneous wettabilities ranging only from 65° to 75°. We note that the static DIW contact angles of PMMA and PHEMA are 75° and 48°, respectively. Our results indicate that on tethered PHEMA-*b*-PMMA diblock layer exposed to a solvent that collapses the top PMMA block the measured DIW contact angle increases with decreasing PMMA block lengths. When correlated with the SFM data, this observation indicates that the areas most prone to rearrangement (exposing the underlying PHEMA layer) are those with higher molecular weight PMMA block. In fact, in the regions of the substrate where we observe a clear transition from M to BC phases, we also detect a rapid decrease in the contact angle, which ranges from $\approx 70°$ to $\approx 50°$. For shorter PMMA (micellar region), the PMMA blocks remain in isolated micelles close to the surface and therefore affect the DIW contact angle readings to indicate a PMMA surface, in agreement with the theoretical prediction of Zhulina and coworkers [33,34]. In the case of longer PMMA (BC region), the interaction of the PMMA blocks to form the bicontinuous structure allows the PMMA phase to remain submerged in the PHEMA layer.

3.2. Triblock copolymer brushes with variable block lengths

In the preceding section we have described the formation and properties of diblock copolymer brush assemblies on solid substrates, where we varied systematically the length of each block in two orthogonal directions. We have demonstrated that such structures are suitable for screening complex interfacial phenomena, such as the morphology development of the brush after exposing to selective solvents. Structures more complex than diblock copolymers may be formed using our dipping method, however. These may involve ABC triblock copolymers with variable lengths of each block; their formation is described in the following section.

In order to carry out a complete investigation of the morphologies and surface behavior of surface-tethered ABC triblocks, one has to systematically vary four independent variables, *i.e.*, the volume fractions of each block and the overall triblock brush thickness. In order to accomplish this, a few modifications to the existing sample preparation design have to be done. First, one has to switch from the orthogonal sample geometry to a triangular specimen arrangement. The new geometry would thus resemble classical ternary phase diagrams (drawn into regular or equilateral triangles) involving 3-component mixtures. In the conventional 3-component mixture cases, say XYZ, each corner of the triangle corresponds to the pure component (X or Y or Z), each side denotes the composition along a given binary alloy (XY, XZ and YZ), and any point inside the triangle marks the composition of the XYZ mixture. The relative proportion of every component of the mixture is given by the lengths on the perpendiculars drawn between the corner
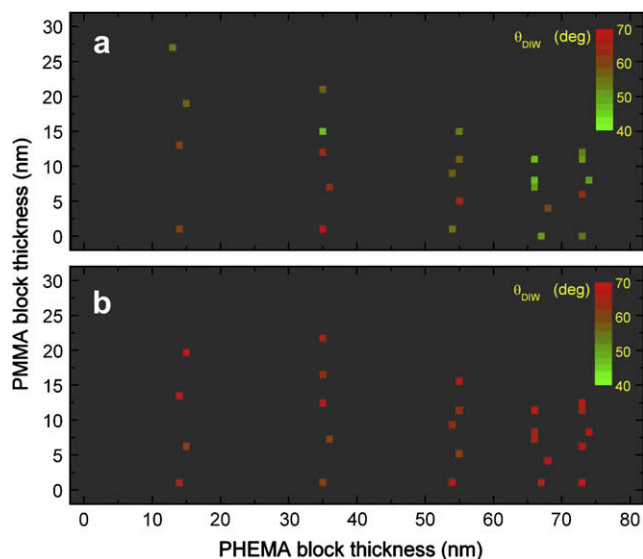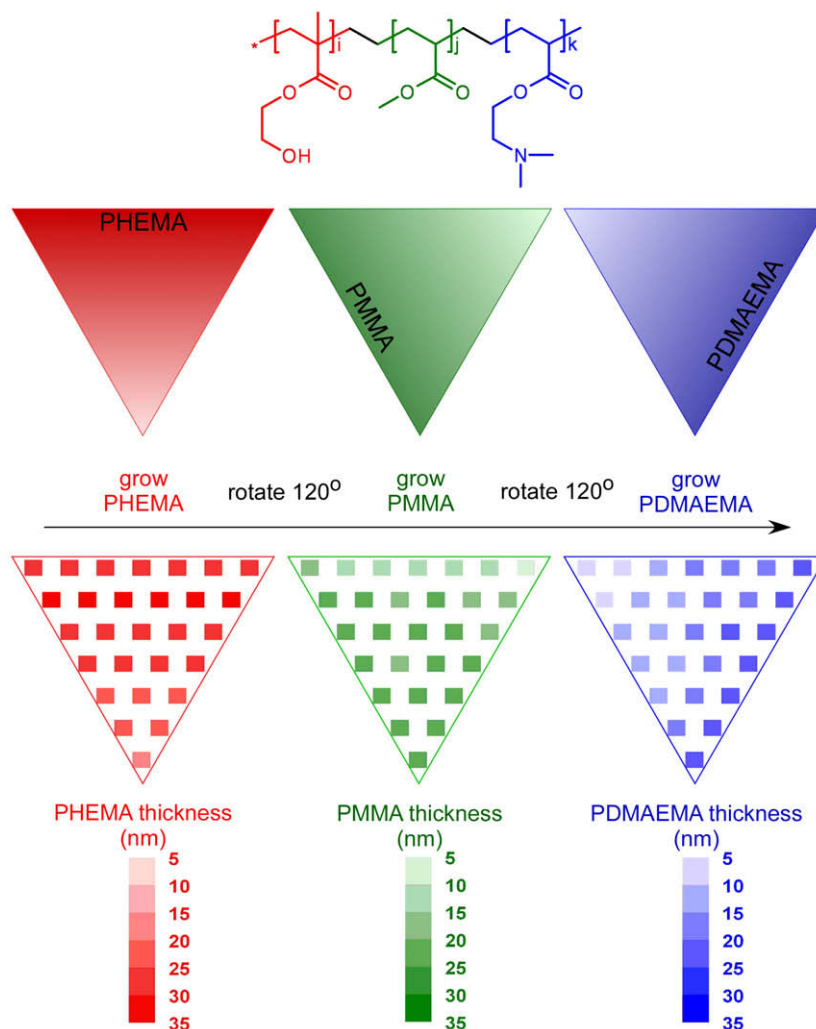
Fig. 10. Formation of triblock copolymer gradient poly[(2-hydroxyethyl methacrylate)-*b*-(methyl methacrylate)-*b*-(dimethylaminoethyl methacrylate)] (PHEMA-*b*-PMMA-*b*-PDMAEMA) with variation of the lengths of all blocks. The top panel depicts the chemical formula of the triblock copolymer. The middle panel shows the intended variation of the block length of each of the blocks. The bottom panel reveals the dry thickness variation of each individual block as measured by ellipsometry on selected positions on the substrate.

and the corresponding opposite side of the triangle. Our triblock copolymer system will be formed on such an equilateral triangle substrate. In order to add the effect of the fourth variable, *i.e.*, the total length of the copolymer, several such triangular samples would have to be generated. There is no simple way to combine the effects of all four variables on a single sample, however. It has to be noted that even with this "slight complication", the suggested combinatorial sample design would still provide much improvement over the conventional "single specimen" approach, thus providing much needed systematized speed of sample preparation and property screening.

As a proof of concept, we have generated, for the first time, such a surface-anchored triblock copolymer assembly of poly[(2-hydroxyethyl methacrylate)-*b*-(methyl methacrylate)-*b*-(dimethylaminoethyl methacrylate)] (PHEMA-*b*-PMMA-*b*-PDMAEMA) with variable lengths of each of the three blocks. Rather than following the conventional approach of having the pure component positioned in each corner of the triangle, the block copolymers are organized such that each pure block occupies one of the edges of the sample and decreases smoothly as one moves in the direction perpendicular to the edge. The middle panel in Fig. 10 depicts pictorially the intended sample design. First, a flat silicon substrate is cut into a triangular shape, and is decorated with the BMPUS initiator. The sample is placed vertically into the dipping gradient

chamber and PHEMA brushes with gradient in molecular weight are formed using the recipe detailed earlier. After the HEMA polymerization, the sample is thoroughly washed, rotated by 120° counterclockwise and molecular weight gradient PMMA brushes are grown from the existing PHEMA macroinitiators by utilizing the dipping apparatus. After the second reaction, the sample is thoroughly washed and again rotated by 120° counterclockwise, after which yet another molecular weight gradient of PDMAEMA is grown from the PMMA macroinitiator centers. The thickness on selected areas on the sample is measured via VASE after each polymerization step. The bottom panel in Fig. 10 shows thickness profiles for each block. The colour variation denotes changes from ≈1 to ≈35 nm on the sample. As indicated by the data in Fig. 10, the lengths of all blocks vary systematically in the three different directions, thus leading to gradual variations in compositions of the entire triblock copolymer. In order to address the effect of the block lengths, one would have to prepare several such specimens, as discussed earlier in the text. Hence, while we are not in the position to make any detailed and systematic studies of the phase behavior of such triblock copolymer brushes, this single example illustrates the capability of the gradient-forming approach. It is our hope that in the near future this approach (or its variant) would be further developed and utilized to gain more insight into the phase behavior of complex and not yet fully understood systems, such as triblock copolymers.

4. Summary and outlook

In this paper we have presented methodologies leading to the fabrication of substrate-bound copolymer assemblies with systematic variation of block lengths. We have demonstrated the application of such strategies on two case studies. In the fist one, we described the formation of surface-tethered poly[(2-hydroxyethyl methacrylate)-*b*-(methyl methacrylate)] (PHEMA-*b*-PMMA) diblock copolymer brushes and used such structures for systematically investigating the morphological transitions of surface topographies upon exposing the PHEMA-*b*-PMMA brushes to solvents that selectively collapse either the top or the bottom block of the diblock copolymer. Using scanning force microscopy we have demonstrated that the observed surface morphologies depend on the length of the bottom and the top block. Structures involving collapsing the top PMMA block comprise either flat (F), micellar (M) or bicontinuous (BC) phases. We have shown that the experimental phase diagram mapping out the occurrence of the three conformations is in agreement with theoretical predictions by Zhulina and coworkers and computer simulations of Yin and coworkers. In the second case study, we have documented the formation of triblock copolymer assemblies of poly[(2-hydroxyethyl methacrylate)-*b*-(methyl methacrylate)-*b*-(dimethylaminoethyl methacrylate)] (PHEMA-*b*-PMMA-*b*-PDMAEMA) brushes with length-independent variations of each block. We have shown that such structure can be built by sequential deposition of polymer brush layers with a gradient of brush length or molecular weight. While we have not demonstrated any particular functionality of the latter structures, we suggest that they can be used as a convenient platform for investigating phase behavior of triblock copolymers. Moving beyond the solvent response, we hypothesize that if a sufficient number of triblock sequences is built in the manner described in this paper, so that "bulk-like" behavior can be recovered, one can, in principle, use such structures for systematically probing systematically phase development of tri-block copolymer melts [43].

References

[1] Zhao B, Brittain WJ. Prog Polym Sci 2000;25:677.
[2] Advincula RC, Brittain WJ, Rühe J, Caster K, editors. Polymer brush. New York: Wiley; 2004.
[3] Edmondson S, Osborne VL, Huck WTS. Chem Soc Rev 2004;33:14.
[4] Brittain WJ, Minko S. J Polym Sci Part A Polym Chem 2007;45:3505.
[5] Zhou F, Huck WTS. Phys Chem Chem Phys 2006;8:3815.
[6] Russell TP. Science 2002;297:964.
[7] Minko S, editor. Responsive polymer materials: design and applications. Blackwell Publishing; 2006.
[8] Luzinov I, Minko S, Tsukruk VV. Prog Polym Sci 2004;29:635.
[9] Minko SJ. Macromol Sci C: Polym Rev 2006;46:397.
[10] Luzinov I, Minko S, Tsukruk VV. Soft Matter 2008;4:714.
[11] Zhao B, Brittain WJ, Zhou W, Cheng SZD. Macromolecules 2000;33:8821.
[12] Zhao B, Brittain WJ, Zhou W, Cheng SZD. J Am Chem Soc 2000;122:2407.
[13] Santer S, Rühe J. Polymer 2004;45:8279.
[14] Santer S, Kopyshev A, Donges J, Rühe J. Polymer 2006;18:2359.
[15] Yu K, Wang HF, Han YC. Langmuir 2007;23:8957.
[16] Xu C, Wu T, Drain CM, Batteas JD, Fasolka MJ, Beers KL. Macromolecules 2006;39:3359.
[17] Wu T, Efimenko K, Genzer J. J Am Chem Soc 2002;124:9394.
[18] Ionov L, Zdyrko B, Sidorenko A, Minko S, Klep V, Luzinov I, et al. Macromol Rapid Commun 2004;25:360.
[19] Mougin K, Ham AS, Lawrence MB, Fernandez EJ, Hillier AC. Langmuir 2005;21:4809.
[20] Y Liu, Klep V, Zdyrko B, Luzinov I. Langmuir 2005;21:11806.
[21] Bhat RR, Tomlinson MR, Genzer J. J Polym Sci Polym Phys Ed 2005;43: 3384.
[22] Wang X, Tu H, Braun PV, Bohn PW. Langmuir 2006;22:817.
[23] Wang X, Bohn PW. Adv Mater 2007;19:515.
[24] Tomlinson MR, Genzer J. Macromolecules 2003;36:3449.
[25] Tomlinson MR, Genzer J. Chem Commun 2003;12:1350.
[26] Xu C, Wu T, Mei Y, Drain CM, Batteas JD, Beers KL. Langmuir 2005;21:11136.
[27] Xu C, Barnes SE, Wu T, Fischer DA, DeLongchamp DM, Batteas JD, et al. Adv Mater 2006;18:1427.
[28] Bhat RR, Tomlinson MR, Wu T, Genzer J. Adv Polym Sci 2006;198:51.
[29] Kim MS, Khang G, Lee HB. Prog Polym Sci 2008;33:138.
[30] Genzer J, Bhat RR. Langmuir 2008;24:2294.
[31] Morgenthaler S, Lee S, Zürcher S, Spencer ND. Soft Matter 2008;4:419.
[32] Tomlinson MR, Genzer J. Langmuir 2005;21:11552.
[33] Zhulina E, Singh C, Balasz AC. Macromolecules 1996;29:6338.
[34] Zhulina E, Singh C, Balasz AC. Macromolecules 1996;29:8254.
[35] Balazs AC, Singh C, Zhulina E, Chern S-S, Lyatskaya Y, Pickett G. Prog Surf Sci 1997;55:181.
[36] Yin Y, Sun P, Li B, Chen T, Jin Q, Ding D, et al. Macromolecules 2007;40: 5161.
[37] Matyjaszewski K, Miller PJ, Shukla N, Immaraporn B, Gelman A, Luokala BB, et al. Macromolecules 1999;32:8716.
[38] Jones DM, Huck WTS. Adv Mater 2001;13:1256.
[39] Chatterjee U, Jewrajka SK, Mandal BM. Polymer 2005;46:1575.
[40] Robinson KL, Khan MA, de Paz Báñez MV, Wang XS, Armes SP. Macromolecules 2001;34:3155.
[41] Tomlinson MR, Efimenko E, Genzer J. Macromolecules 2006;39:9049.
[42] The molecular weight of the brush (M) can be estimated from the dry brush thickness (*h*) from $M \approx 1200\,h$, where *M* is in Daltons and *h* is in nanometers. This approximate relation has been obtained by growing chains simultaneously in bulk and on the surface and determining *M* via size exclusion chromatography and *h* via ellipsometry. Although it has been found to be valid for a range of methacrylates and acrylates grown from BMPUS initiator layers deposited under identical conditions, this relationship should be considered as an estimate only because it assumes that chains grown under confinement possess the same rate of polymerization as those polymerized in solution. Nevertheless, this relationship provides a very reasonable estimate for the chain grafting density (σ): $\sigma \approx 0.45$ chains/nm^2.
[43] Bates F, Fredrickson G. Phys Today 1999;52:32.